Current Optics and Photonics
Vol. 2, No. 2, April 2018, pp. 147-152

ISSN: 2508-7266(Print) / ISSN: 2508-7274(Online)
DOI: https://doi.org/10.3807/COPP.2018.2.2.147

Numerical Study of a Novel Bi-focal Metallic Fresnel Zone Plate Having Shallow Depth-of-field Characteristics

Jinseob Kim[1], Juhwan Kim[1], Jeongkyun Na[1], and Yoonchan Jeong[1,2]*

[1]*Laser Engineering and Applications Laboratory, Department of Electrical and Computer Engineering, Seoul National University, Seoul 08826, Korea*
[2]*ISRC & IAP, Seoul National University, Seoul 08826, Korea*

(Received March 15, 2018 : revised March 20, 2018 : accepted March 20, 2018)

We propose a novel bi-focal metallic Fresnel zone plate (MFZP) with shallow depth-of-field (DOF) characteristics. We design the specific annular slit patterns, exploiting the phase-selection-rule method along with the particle swarm optimization algorithm, which we have recently proposed. We numerically investigate the novel characteristics of the bi-focal MFZP in comparison with those of another bi-focal MFZP having equivalent functionality but designed by the conventional multi-zone method. We verify that whilst both bi-focal MFZPs can produce dual focal spots at 15 μm and 25 μm away from the MFZP plane, the former exhibits characteristics superior to those of the latter from the viewpoint of axial resolution, including the axial side lobe suppression and axial DOF shallowness. We expect the proposed bi-focal MFZP can readily be fabricated with electron-beam evaporation and focused-ion-beam processes and further be exploited for various applications, such as laser micro-machining, optical trapping, biochemical sensing, confocal sensing, etc.

Keywords : Metallic Fresnel zone plates, Bi-focusing, Depth of field, Numerical modeling
OCIS codes : (080.3630) Lenses; (240.3990) Micro-optical devices; (050.1380) Binary optics

I. INTRODUCTION

Since a zone plate was first devised by Fresnel [1], a variety of different types of zone plates, i.e., so-called Fresnel zone plates (FZPs), have been studied as a novel focusing element having exotic diffraction characteristics [2-4]. Moreover, since thin metallic structures can readily be implemented onto a fiber facet as well as onto a flat optical substrate, novel characteristics of metallic FZPs (MFZPs) can also open up great opportunities for various fiber-optic applications [5-7], which inherently have very high compactness and stability. In recent years, exploitations of FZP structures into bi-focusing applications have been attracting a considerable amount of research attention. These applications include multi-zone FZPs, Fibonacci diffractive lenses, and Thue-Morse zone plates to name a few [8-10]. However, most schemes hit various technical issues such as having difficulties in keeping longitudinal focusing sharpness, generating focal spots at desired locations, or suppressing undesirable side lobes [11, 12]. In particular, the loss of longitudinal focusing sharpness can severely degrade the performance of a bi-focal lens, particularly, in sensing or laser-based micro-machining applications [13, 14], which invariably require a high axial resolution. On the other hand, we have recently proposed a novel systematic design method based on the phase selection rule (PSR) for multi-focal MFZPs, reporting a preliminary simulation result based on it [15]. Although we did show that the method would have great potential as a systematic design method for multi-focal MFZPs, it has remained unanswered whether the method is capable of resolving the aforementioned issues incurred from the existing technologies to a satisfactory level, particularly, when the method is utilized for designing a bi-focal MFZP having shallow depth-of-field (DOF) characteristics.

*Corresponding author: yoonchan@snu.ac.kr, ORCID 0000-0001-9554-4438
Color versions of one or more of the figures in this paper are available online.

Therefore, in this paper we utilize the PSR method for optimally designing a bi-focal MFZP and discuss its functional characteristics, including the precision of focal spots, the sharpness of the longitudinal focusing, and the suppression ratio of axial side lobes, from the viewpoint of axial resolution. We also discuss and verify the capability and feasibility of the PSR method in comparison with those of a benchmarking MFZP having equivalent bi-focal functionality but designed by the conventional multi-zone method.

II. DESIGN AND OPTIMIZATION

The PSR method is based on the time-reversal characteristic and superposition principle of electromagnetic waves [15, 16], which can be explained briefly as follows: Let us suppose that there is an MFZP at $z=0$ that produces dual focal spots at $z=z_1$ and $z=z_2$ when a plane electromagnetic wave is incident onto it at normal incidence. In a reciprocal manner, if one places two virtual point sources (VPSs) at the dual focal points at $z=z_1$ and $z=z_2$, respectively, spherical electromagnetic waves generated by the VPSs will in turn produce a phase profile at the MFZP plane, i.e., at $z=0$. One can quantize the phase profile in a binary manner into ϕ_+ and ϕ_- such that $0 \le \phi_+ < \pi$ and $\pi \le \phi_- < 2\pi$, based on the so-called PSR. This quantization procedure results in a binary $\phi_+ - \phi_-$ profile in an annular format because of the axial symmetry. If one assumes from a viewpoint of relative phase difference that the electromagnetic waves in the ϕ_+ regions originally radiated from VPSs are in phase at $z=0$, the electromagnetic waves in the ϕ_- regions can be regarded out of phase at $z=0$. Then, if one makes the ϕ_+ regions open and the ϕ_- regions closed and illuminates the MFZP with a plane electromagnetic wave from the other side, the electromagnetic waves that pass through the opening of the annular slit structure will result in being in phase at $z=z_1$ and $z=z_2$, because of the time-reversal characteristic of electromagnetic waves. Since all the possible paths for being out of phase at $z=z_1$ and $z=z_2$ are inherently prohibited by blocking the ϕ_- regions at the MFZP plane, the electromagnetic waves started from the ϕ_+ regions will invariably interfere at $z=z_1$ and $z=z_2$ constructively, thereby leading to forming dual focal spots there. In fact, if one uses a single VPS, the resultant annular slit structure will become exactly the same as the form of a conventional MFZP, which is formulated by [7]:

$$r_n = \sqrt{(n+\alpha)\lambda_0 f_0 + \frac{(n+\alpha)^2\lambda_0^2}{4}} \; (n=1, 2, \cdots, 2N), \qquad (1)$$

where r_n denotes the inner radius of an annular-slit opening for an odd integer n or its outer radius for an even integer n, N the total number of annular slits, α the initial phase-offset constant, f_0 the focal length, and λ_0 wavelength of incident light.

Therefore, all one has to do is to define the VPSs in an appropriate manner. In fact, they can be represented by their complex amplitudes, so that one just needs to choose their absolute amplitudes (or intensities) and initial phases. In general, as can be seen from Eq. (1), a conventional MFZP can be designed in a variety of forms depending on the choice of the initial phase-offset value α. Similarly, a bi-focal MFZP to be designed by the PSR method can also be of different forms, depending on the choice of the complex amplitudes of the VPSs. Therefore, one can determine an optimal one of them such that the resultant MFZP satisfactorily acquires all the desired characteristics as closely as possible. For this purpose, we additionally choose to use the particle swarm optimization (PSO) algorithm [17], although it is not the only method for the optimization procedure.

III. NUMERICAL RESULTS AND DISCUSSION

In this section, we implement the PSR method in designing a bi-focal MFZP and numerically characterize its functional characteristics. In addition, we also design another bi-focal MFZP for comparison, using the multi-zone method that is one of the most frequently used design methods for bi-focal MFZPs [8]. Based on both results we comparatively discuss the distinct characteristics between the two bi-focal MFZPs, also verifying the superiority of the PSR method to the conventional multi-zone method.

The simulation conditions for both bi-focal MFZPs are as follows: We set the diameters of the MFZPs to be 50 μm, considering the use of them on an optical fiber platform [18-20]. We assume that the dual focal spots of an identical peak intensity level are formed at $z=15$ μm and $z=25$ μm for normal incidence of a plane electromagnetic wave at 650 nm. We utilize a commercial computational tool based on Matlab (R2016b, MathWorks) for both design and optimization procedures. In particular, we assume that the minimal step of the annular slit structure in the radial direction is fixed to 50 nm, taking account of a typical resolution of the focused-ion-beam (FIB) process for fabrication [21, 22]. During the PSO procedure, we take the following three indicators as the criteria for optimization: (1) how exactly the two foci are formed at the desired locations in terms of $\triangle f_m$, (2) how evenly the peak intensities of the two focal spots are determined in terms of $\triangle I$, and (3) how effectively the axial side lobes are suppressed in terms of $\triangle S$. Using penalty parameters with these three criteria, we iteratively perform the PSO procedure until all three parameters reach the corresponding target tolerance values as closely as they can, as summarized in Table 1.

First, the graphics shown in Fig. 1 illustrate the simulation results regarding the shape of the MFZP designed by the PSR method and its resultant transmission characteristics when a plane electromagnetic wave at 650 nm is incident onto it. It is worth noting that in Fig. 1(b) all the intensity levels are normalized to the maximum value of all. One can clearly see that bi-focal peaks of nearly identical intensities are formed at the targeted locations at $z = 15$ μm and $z = 25$ μm: The dual focal spots are formed at 14.95 μm and 25.05 μm. Thus, the corresponding relative focal point mismatch values are given by 0.33% and 0.20%, respectively. The intensities of the bi-focal peaks are sufficiently even, exhibiting a relative intensity mismatch of 0.17% with respect to their average value. Finally, the side lobe suppression ratio is given by -9.42 dB, which slightly misses the target value of -10 dB. In general, MFZPs inherently exhibit super-oscillatory behaviors in the near side, often producing higher-order focal spots beside the fundamental one [23, 24], so that we suspect that complete suppression of such peaks remains inherently cumbersome and challenging. Notwithstanding, we stress that in the given conditions, the characteristics of the bi-focal MFZP are sufficiently satisfactory in terms of the specified tolerance values as summarized in Table 1.

On the other hand, we also investigate the conventional multi-zone method for designing another bi-focal MFZP having all equivalent bi-focal functionality. In fact, the method divides the whole area of the MFZP into inner and outer regions, i.e., Zone 1 and Zone 2, individually determining the annular slit structure for each zone via Eq. (1). The inner region, i.e., Zone 1, is designed to produce a shorter focal point from the viewpoint of the balanced axial resolution between the dual focal spots. In addition, it is worth noting that while we use the multi-zone method, we additionally exploit the PSO algorithm in determining the diameter that divides the whole area of the MFZP into Zone 1 and Zone 2, and the two phase-offset values for Zone 1 and Zone 2, i.e., $\alpha 1$ and $\alpha 2$, in order that the characteristic properties of the MFZP satisfy the tolerance values specified in Table 1 as much as possible. This is for the sake of fair comparison between the results by the two different methods, i.e., the PSR method and the conventional multi-zone method.

The graphics shown in Fig. 2 illustrate the resultant MFZP pattern and its corresponding transmission characteristics. It is worth noting that in Fig. 2(b) all the intensity levels are normalized to the maximum value of all; however, if the incident condition were the same as in Fig. 1(b), the actual

TABLE 1. Target design parameters of bi-focal MFZP with shallow DOF characteristics

Design parameters

Parameters	Foci	Wavelength	Diameter	Slit resolution	Tolerance		
					Position $\lvert \triangle f_{1,2} \rvert$	Intensity $\lvert \triangle I \rvert$	Side-lobe peak $\triangle S$
Value	15, 25 μm	650 nm	50 μm	50 nm	1%	1%	-10 dB

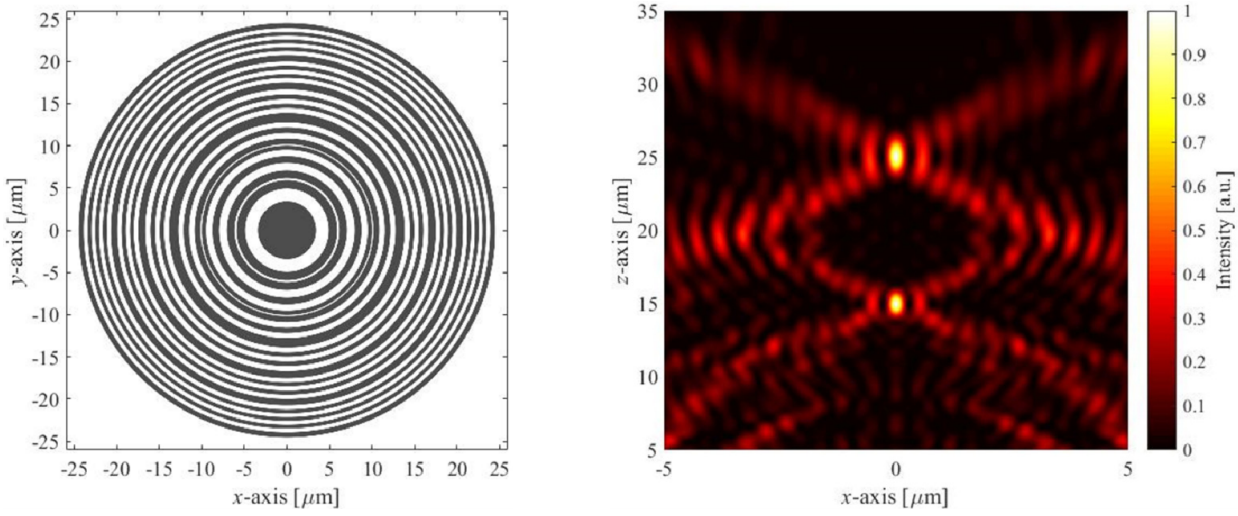

(a) (b)

FIG. 1. Simulation results on the bi-focal MFZP designed by the PSR method according to the target parameters specified in Table 1: (a) Annular slit pattern of the designed bi-focal MFZP. (b) Calculated intensity distribution formed through the PRS-based bi-focal MFZP.

peak intensity level should be reduced to 82.5% of the peak intensity level shown in Fig. 1(b). One can see that the MFZP by the multi-zone method can also produce bi-focal peaks, such that $z_1 = 15.10$ μm and $z_2 = 24.85$ μm, which give rise to the relative focal point mismatch values are given by 0.67% and 0.60%, respectively. These values are satisfactory in terms of the given tolerance value specified in Table 1. The relative intensity mismatch is given by 0.33%, which is also satisfactory as specified in Table 1. However, the obtained axial side-lobe suppression ratio is only given by -6.81 dB at best, which is significantly off the target tolerance value, in contrast to the case with the PSR method. Apart from such characteristics, the overall background intensity levels are relatively high in comparison with those by the PSR method as shown in Fig. 1(b).

In addition, paying more attention to the axial resolution, we plot the transmitted beam patterns on the *z*-axis for both bi-focal MFZPs in Fig. 3 at the same time, in which we assume that the incident electromagnetic waves have the same intensity levels. One can clearly see that the axial resolutions obtained by the PSR method are significantly superior to those by the conventional multi-zone method at both focal points. Firstly, the axial side-lobe suppression ratio obtained by the former is -9.42 dB, whereas that by the latter is -6.81 dB, which means the former can lead to twice better performance than the latter in terms of axial

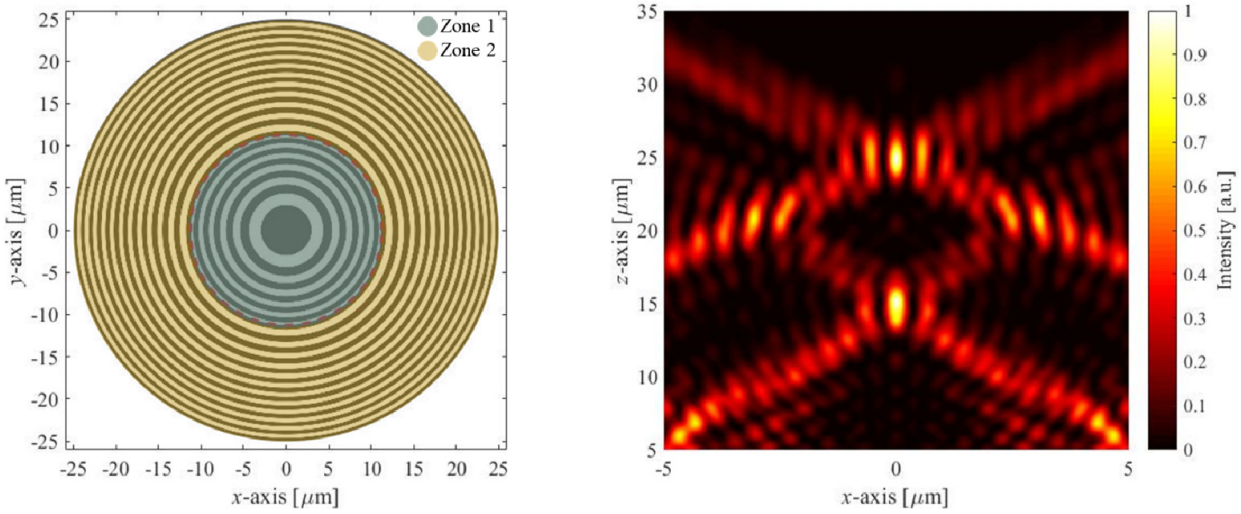

(a) (b)

FIG. 2. Simulation results on the bi-focal MFZP designed by the multi-zone method according to the target parameters specified in Table 1. (a) Annular slit pattern of the designed bi-focal MFZP. Zone 1 and Zone 2 are respectively designed according to Eq. (1) for forming the dual focal spots at 15 and 25 μm. (b) Calculated intensity distribution formed through the multi-zone based bi-focal MFZP.

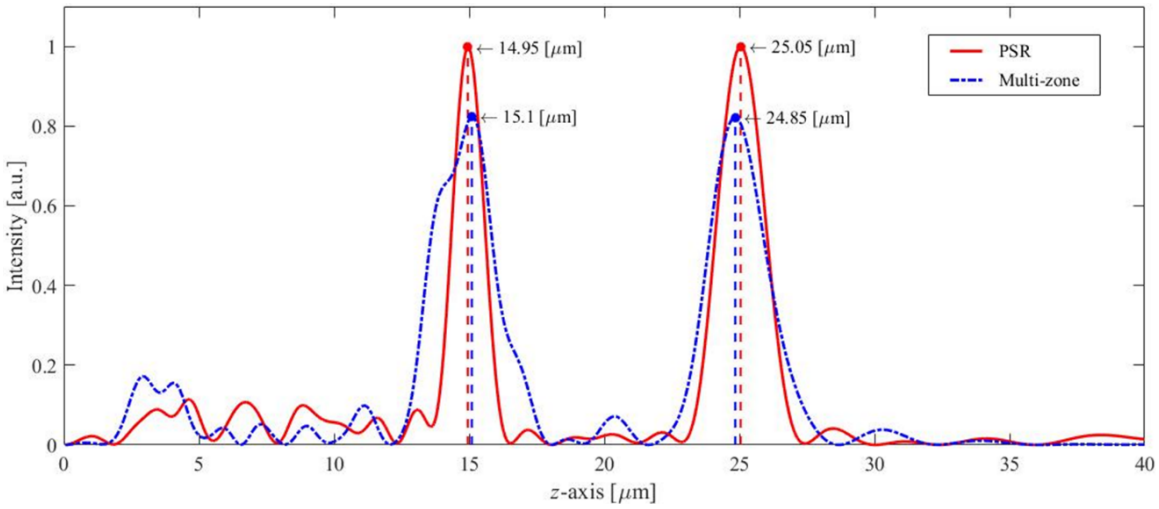

FIG. 3. Axial intensity profiles formed though the PSR-based bi-focal MFZP and the multi-zone bi-focal MFZP. Red trace: PSR-based bi-focal MFZP. Blue trace: multi-zone bi-focal MFZP. Note that the incident conditions are assumed to be identical.

side-lobe suppression. Secondly, the DOF values at z_1 and z_2 obtained by the former are 1.32 μm and 1.99 μm in full width at half maximum (FWHM), respectively, whereas those by the latter are 2.64 μm and 2.46 μm (FWHM), respectively. Consequently, it is worth noting that the DOF values at z_1 and z_2 obtained by the former are only 50.1% and 80.8% of those by the latter, respectively. That is, the bi-focal MFZP by the former can lead to significantly shallower DOF characteristics than those by the latter, thereby resulting in significantly enhanced axial resolutions. Consequently, the peak intensity levels by the former are significantly higher than those by the latter. Thirdly, we note that the focal spots obtained by the former are more axially symmetric than those by the latter. The overall characteristics are summarized in the Table 2, from which one can readily notice the superiority of the PSR method to the conventional multi-zone method.

IV. CONCLUSION

We have proposed a novel bi-focal MFZP having shallow DOF characteristics, for which we exploited the PSR method along with the PSO algorithm. We performed numerical simulations to characterize its bi-focal functionality with normal incidence of a plane electromagnetic wave at 650 nm, in comparison with another bi-focal MFZP designed by the conventional multi-zone method. We verified that whilst both MFZPs can produce bi-focal spots at the desired locations, i.e., at z_1 = ~15 μm and z_2 = ~25 μm, their specific characteristics are significantly distinct, particularly, from the perspective of axial resolution: The PSR-based MFZP can lead to significantly better characteristics in terms of the axial side lobe suppression ratio and the axial DOF values at the given dual focal points (see Table 2 for more details). These consequences are mainly due to the fact that the multi-zone method inevitably leads to loss of the effective aperture size allocated for each focal spot, whereas the PSR method can keep the full aperture size for each focal spot regardless of the number of focal spots it produces. Thus, the PSR method can become even further advantageous as the number of focal spots increases. Although we have verified the feasibility of the PSR method and the bi-focal MFZP, we think that there is room for improvement from the viewpoint of the numerical optimization procedure: One can further investigate even higher numerical resolution or different optimization algorithms for it. We expect that the proposed bi-focal MFZP can be exploited for various applications such as laser micromachining, optical trapping, biochemical sensing, confocal sensing, etc., which invariably require high axial resolution.

ACKNOWLEDGEMENT

This study was supported by National Research Foundation of Korea (NRF) grant funded by the government of Korea (2017R1D1A1B03036201); Ministry of Trade, Industry and Energy (Project no. 10060150); Brain Korea 21 Plus Program.

REFERENCES

1. A. J. Fresnel, "Calcul de l'intensite de la lumiere au centre de l'ombre d'un ecran et d'une ouverture circulaires eclairee par une point radieux," Oeuvres d'Augustin Fresnel **1**, 365-372 (1866).
2. M. Young, "Zone plates and their aberrations," J. Opt Soc Am. **62**, 972-976 (1972).
3. G. Saavedra, W. D. Furlan, and J. A. Monsoriu, "Fractal zone plates." Opt. Lett. **28**, 971-973 (2003).

TABLE 2. Optimized parameters and resultant characteristics of bi-focal MFZPs designed by the PSR method and the multi-zone method

Optimized parameters (PSR)

Parameters	Relative intensities (I_1, I_2)	Initial phase-offset (ϕ_1, ϕ_2)	Position $\lvert\triangle f_{1,2}\rvert$	Intensity $\lvert\triangle I\rvert$	Side-lobe peak $\triangle S$
Value	0.424, 1	1.303 π, 1.677 π	< 0.33%	< 0.17%	< -9.42 dB

Optimized parameters (Multi-zone)

Parameters	Radius of zone boundary	Initial phase-offset (α_1, α_2)	Position $\lvert\triangle f_{1,2}\rvert$	Intensity $\lvert\triangle I\rvert$	Side-lobe peak $\triangle S$
Value	11.25 μm (6th slit)	0.365, 0.559	< 0.67%	< 0.33%	< -6.81 dB

Comparison of results

Parameters / Methods	Foci (f_1, f_2)	Depth of field at f_1 and f_2	Relative peak intensities at f_1 and f_2
PSR	14.95, 25.05 μm	1.32, 1.99 μm	0.998, 1.000
Multi-zone	15.10, 24.85 μm	2.64, 2.46 μm	0.825, 0.822

4. J. Jia, C. Xie, M. Liu, and L. Wan, "A super-resolution Fresnel zone plate and photon sieve," Opt. Lasers Eng. **48**, 760-765 (2010).
5. R. S. R. Ribeiro, P. Dahal, A. Guerreiro, P. A. Jorge, and J. Viegas, "Fabrication of Fresnel plates on optical fibres by FIB milling for optical trapping, manipulation and detection of single cells," Sci. Rep. **7**, 4485 (2017).
6. H. Kim, H. An, J. Kim, S. Lee, K. Park, S. Lee, S. Hong, L. A. Vazquez-Zuniga, S. Y. Lee, B. Lee, and Y. Jeong, "Corrugation-assisted metal-coated angled fiber facet for wavelength-dependent off-axis directional beaming," Opt. Express **25**, 8366-8385 (2017).
7. H. Kim, J. Kim, H. An, Y. Lee, G. Y. Lee, J. Na, K. Park, S. Lee, S. Y. Lee, B. Lee, and Y. Jeong, "Metallic Fresnel zone plate implemented on an optical fiber facet for super-variable focusing of light," Opt. Express **25**, 30290-30303 (2017).
8. M. J. Simpson and A. G. Michette. "Imaging properties of modified Fresnel zone plates," Opt. Acta **31**, 403-413 (1984).
9. J. A. Monsoriu, A. Calatayud, L. Remón, W. D. Furlan, G. Saavedra, and P. Andrés, "Bifocal Fibonacci diffractive lenses," IEEE Photonics J. **5**, 3400106 (2013).
10. V. Ferrando, F. Giménez, W. D. Furlan, and J. A. Monsoriu, "Bifractal focusing and imaging properties of Thue-Morse Zone Plates," Optics Express **23**, 19846-19853 (2015).
11. Q. Zhang, J. Wang, M. Wang, J. Bu, S. Zhu, B. Z. Gao, and X. Yuan, "Depth of focus enhancement of a modified imaging quasi-fractal zone plate," Opt. Laser Technol. **44**, 2140-2144 (2012).
12. Q. Q. Zhang, J. G. Wang, M. W. Wang, J. Bu, S. W. Zhu, R. Wang, B. Z. Gao, and X. C. Yuan, "A modified fractal zone plate with extended depth of focus in spectral domain optical coherence tomography," J. Opt. **13**, 055301 (2011).
13. J. Huang, M. Yuichi, and F. Yamamoto, "Shallow DOF-based particle tracking velocimetry applied to horizontal bubbly wall turbulence," Flow Meas. Instrum. **19**, 93-105 (2008).
14. K. Venkatakrishnan and B. Tan, "Interconnect microvia drilling with a radially polarized laser beam," J. Micromech. Microeng. **16**, 2603 (2006).
15. J. Kim, H. Kim, K. Park, and Y. Jeong, "Simulation of metallic Fresnel zone plates for axial bi-focusing," in *Proc. The 24th Conference on Optoelectronics and Optical Communications* (Busan, Korea, June 2017), WP-G-1.
16. G. Lerosey, J. De Rosny, A. Tourin, A. Derode, G. Montaldo, and M. Fink, "Time reversal of electromagnetic waves," Phys. Rev. Lett. **92**, 193904 (2004).
17. J. Kennedy and R. Eberhart, "Particle swarm optimization," in *Proc. IEEE International Conference on Neural Networks. IV.* (Perth, WA, Australia, 27 Nov.-1 Dec. 1995), pp. 1942-1948.
18. P. Pepeljugoski, M. J. Hackert, J. S. Abbott, S. E. Swanson, S. E. Golowich, A. J. Ritger, P. Kolesar, Y. C. Chen, and P. Pleunis, "Development of system specification for laser-optimized 50-μm multimode fiber for multigigabit short-wavelength LANs," J. Lightwave Technol. **21**, 1256 (2003).
19. P. Sillard, D. Molin, M. Bigot-Astruc, A. Amezcua-Correa, K. de Jongh, and F. Achten, "50 μm multimode fibers for mode division multiplexing," J. Lightwave Technol. **34**, 1672-1677 (2016).
20. A. S. Kurkov, E. M. Sholokhov, and Y. E. Sadovnikova, "All-fiber supercontinuum source in the range of 1550-2400 nm based on telecommunication multimode fiber," Laser Phys. Lett. **8**, 598 (2011).
21. R. S. R. Ribeiro, P. Dahal, A. Guerreiro, P. A. Jorge, and J. Viegas, "Fabrication of Fresnel plates on optical fibres by FIB milling for optical trapping, manipulation and detection of single cells," Sci. Rep. **7**, 4485 (2017).
22. E. J. R. Vesseur, R. De Waele, H. J. Lezec, H. A. Atwater, F. J. García de Abajo, and A. Polman, "Surface plasmon polariton modes in a single-crystal Au nanoresonator fabricated using focused-ion-beam milling," Appl. Phys. Lett. **92**, 083110 (2008).
23. M. H. Horman and H. H. M. Chau, "Zone plate theory based on holography," Appl. Opt. **6**, 317-322 (1967).
24. H. H. M. Chau, "Zone plates produced optically," Appl. Opt. **8**, 1209-1211 (1969).